Electronic Supplementary Information

Manganese porphyrin-double strand DNA complex guided in-situ deposition of polyaniline for electrochemical thrombin detection

Shunbi Xie, Yaqin Chai*, Yali Yuan and Ruo Yuan*

Experimental section

Reagents and apparatus

Thrombin (TB), hemoglobin (Hb), hexanethiol (96%, HT), Mn(III)meso-Tetra(N-methyi-4-pyridyl)porphine (MnTMPyP), dopamine (DA), palladium potassium chloride (K_2PdCl_6), chloro platinic acid (H_2PtCl_6), gold chloride ($HAuCl_4$), bovine serum albumin (BSA), human IgG, lysozyme, poly(vinyl pyrrolidone) (PVP, MW ≈ 55 000), sodium citrate (CA), L-ascorbic acid (AA) were purchased from Sigma (St. Louis, MO, USA). Tris-hydroxymethylaminomethane hydrochloride (Tris) was obtained from Roche (Switzerland). $K_3[Fe(CN)_6]$ and $K_4[Fe(CN)_6]$ were purchased from Beijing Chemical Reagent Co. (Beijing, China). The gold nanoparticles (NanoAu, 16 nm) were prepared according to the literature [1]. The HPLC-purified DNA oligonucleotides were purchased from Sangon Biotech Co., Ltd. (Shanghai, China) with the sequences listed as follows:

TBAI: 5'-NH_2-$(CH_2)_6$-GGTTGGTGTGGTTGG-3'

TBAII: 5'-NH_2-$(CH_2)_6$-AGTCCGTGGTAGGGCAGGTTGGGGTGACT-3'

S1: 5'-NH_2-AGAATTGTACTTAAACACCTT-3'

S2: 5'-AAGGTGTTTAAGTACAATTCT-3'

20 mM Tris-HCl buffer (pH 7.4) containing 140 mM NaCl, 5 mM KCl, 1 mM $CaCl_2$ and 1 mM $MgCl_2$ was used as a binding buffer. Phosphate-buffered solution (PBS) (pH 7.0, 0.1 M) containing 10 mM KCl, 2 mM $MgCl_2$ was used as working buffer solution. All other chemicals were of analytical grade and used as received.

Protein solutions were stored at 4 °C before use. Double distilled water was used throughout this study.

All electrochemical measurements, including cyclic voltammetry (CV), differential pulse voltammograms (DPV) were performed with a CHI 660D electrochemical workstation (Shanghai Chenhua Instrument, China). The pH measurements were finished with a pH meter (MP 230, Mettler-Toledo, Switzerland). The scanning electron micrographs were taken with scanning electron microscope (SEM, S-4800, Hitachi, Japan). X-ray photoelectron spectroscopy (XPS) measurements were carried out using a VG Scientific ESCALAB 250 spectrometer (Thermoelectricity Instruments, USA) and using Al Ka X-ray (1486.6 eV) as the light source. A three-electrode system contained a modified glassy carbon electrode (GCE, Φ=4 mm) as working electrode, a platinum wire as auxiliary electrode and a saturated calomel electrode (SCE) as reference electrode.

Electrochemical measurements

All electrochemical experiments were carried out in a conventional electrochemical cell containing a three-electrode arrangement. CVs of the electrode fabrication were performed in 2 mL 5 mM $K_3[Fe(CN)_6]$ and $K_4[Fe(CN)_6]$ solution containing 0.2 M KCl, scanning from -0.6 V to 0.2 V at a scan rate of 100 mV/s. Electrochemical impedance spectroscopy (EIS) was carried out in 2 mL 5 mM $K_3[Fe(CN)_6]$ and $K_4[Fe(CN)_6]$ solution containing 0.2 M KCl with the frequencies swept from 0.1 to 10^5 Hz. The DPV measurement was taken: the potential range was from -0.5 to 0 V, modulation amplitude was 0.05 V, pulse width was 0.05 s, and sample width was 0.0167 s.

Synthesis of Pd@Pt alloy nanocages

Firstly, the Pd@Pt alloy nanocages were synthesized according the reference with some modification[2]. In a typical synthesis, 8.0 mL of an aqueous solution containing 105 mg of PVP, 60 mg of AA, 600 mg KBr and 185 mg KCl was placed in a vial and preheated to 80 °C under magnetic stirring for 10 min. Subsequently, 3.0 mL of an aqueous solution containing 57 mg of K_2PdCl_4 was added with a pipet. After the vial had been capped, the reaction was allowed to continue at 80 °C for 3 h.

The resulted product was collected by centrifugation, washed three times with water to obtain the Pd nanocubes, and redispersed in 10 mL of water. And then, 1 mL of the Pd nanocubes and 7 mL of an aqueous solution containing 33.3 mg of PVP, 300 mg of KBr, and 300 mg of AA were mixed in a glass vial. The mixture was heated to 90 °C in air under magnetic stirring. Meanwhile, l mL of H_2PtCl_4 was then injected into the above solution at a rate of 1 mL/min. The reaction mixture was then heated to 90 °C for 12 h in air. Finally, the solution was centrifuged and washed three times with water to remove PVP, and the obtained Pd@Pt alloy nanocages were redispersed in 2 mL of water.

Synthesis of Pd@Pt/PDA/Au nanocomposites

The Pd@Pt/PDA/Au nanocomposites were synthesized as the following steps. Briefly, 100 mg dopamine hydrochloride and 2 mL Pd@Pt alloy nanocages were added into 2 mL deionized water (pH was approximately 6.0) and dispersed by sonication for 1 min in water bath. This mixture was shaken for 1 h at room temperature. Then 8 mL of 0.1 M Tris-HCl buffer (pH 8.5) was added into the above mixture, and the solution was incubated for 24 h at room temperature under shaking. Then the products were also collected by centrifugation. Finally, the Pd@Pt/PDA aqueous solution was mixed with 1 mL $HAuCl_4$ aqueous solution (1% *wt*) and 1 mL sodium citrate aqueous solution (10% *wt*) stirred overnight at room temperature to obtain Pd@Pt/PDA/Au nanocomposites.

Preparation of the Pd@Pt/PDA/Au-TBA II-S1-BSA bioconjugates

Immobilization of S1 and TBA II onto the as-prepared Pd@Pt/PDA/Au nanocomposites *via* the interaction between Au and -NH_2 was completed according to the following steps: firstly, 2 mL of the as-prepared Pd@Pt/PDA/Au dispersion was mixed with 20 μL TBA II (100 μM) and 20 μL S1 (100 μM) and set on a shaker at 4 °C for 16 h followed by centrifuged. After discarding the supernatant, the mixture was dispersed in 2 mL of PBS (pH 7.0). Subsequently, 1 mg BSA was added into the solution to block the unmodified portion of the nanocomposites for 1 h. After washing by centrifugation, the obtained bio-conjugates were then dispersed in 1 mL PBS (0.1 M, pH 7.0) and stored at 4 °C for further use. For the comparison of performance

based on different labeled probes, the NanoAu (16 nM) labeled TBA II and S1, Pd@Pt nanocages labeled TBA II and S1 were prepared in a similar way.

The fabrication of the sandwich-type aptasensors and the deposition of PANI

Prior to use, GCE was polished carefully with 0.05 and 0.3 μm alumina powder and then washed ultrasonically in water and ethanol for a few minutes. Firstly, gold nanoparticles (AuNPs) were deposited onto the GCE in 1% $HAuCl_4$ solution at the potential of -0.2 V for 30 s. Then the modified electrodes were incubated 20 μL TBAI (2 μM) for 16 h. Subsequently, the resulting electrode was rinsed thoroughly to remove the physically absorbed TBA I and incubated in 20 μL HT (1.0 mM) for 45 min to eliminate nonspecific binding. The fabrication of sandwich format consists of the following two steps. First, the as-prepared electrodes were incubated for 1 h with various concentrations of TB in Tris-HCl buffer (pH 7.4) for protein-aptamer interaction at room temperature. Then 20 μL of the prepared Pd@Pt/PDA/Au-TBA II-S1-BSA bioconjugates were dropped onto the electrode surface and incubated for 1 h. After that, the aptasensors were washed extensively to remove unbounded labels. Second, for the assembly of the MnTMPyP-dsDNA complex on Pd@Pt/PDA/Au surface, the obtained electrodes were incubated with 20 μL of the mixture composed by 2.0 μM S1, 2.0 μM S2, 3 μM MnTMPyP and reacted for 2 h at room temperature.

To perform the deposition of PANI on the MnTMPyP-dsDNA complex, the above modified electrodes were immersed into 0.1 M HAc-NaAc solution (pH 4.6) containing 20 mM aniline and 4 mM H_2O_2 for a desirable accumulation time (30 min) to complete the polymerization reaction. After that, the electrodes were washed with double distilled water and prepared for electrochemical measurement.

Results and discussion

Characteristics of the different nanomaterials

The size and morphology of the as synthesized nanomaterials were characterized by scanning electron microscope (SEM). As shown in Fig. S1A, the cube-like morphology suggested the successful preparation of Pd nanocubes (a). The obtained

Pd-Pt nanocages still had a cubic shape, with a slightly larger size than that of the original Pd cubes, which are quite similar to the previous reports[2] (b). After coated with PDA, a glue-liked morphology wrapped the Pd-Pt nanocages (c). After the Pd@Pt/DA was treated in a solution containing $HAuCl_4$ and sodium citrate, a large amount of Au nanoparticles were clearly observed on the PDA surface (d), indicating that the Pd@Pt/PDA/Au nanocomposites was successfully synthesized. X-ray photoelectron spectroscopy (XPS) analysis provided effective information on the chemical composition of as-prepared Pd@Pt/PDA/Au nanocomposites. The characteristic peaks for Pt4f, Au4f, Pd3d, C1s, N1s and O1s core level regions could be obviously observed at the Pd@Pt/PDA/Au nanocomposites in Fig.S1B, curve a. The nanocomposites displays the spectrum of Pt4f and Pd3d suggesting the successfully synthesis of Pd@Pt nanocages. The C1s, N1s and O1s core level were mainly derived from the PDA. And the Au4f core level indicated that the PDA has anchored Au effective. The spectrum of Pt (b), Au (c) and Pd (d) was also displayed clearly in Fig.S1B.

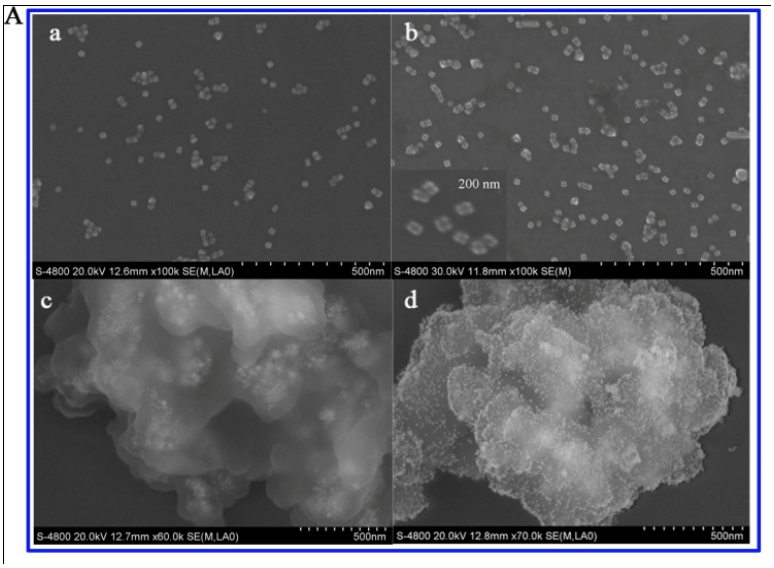

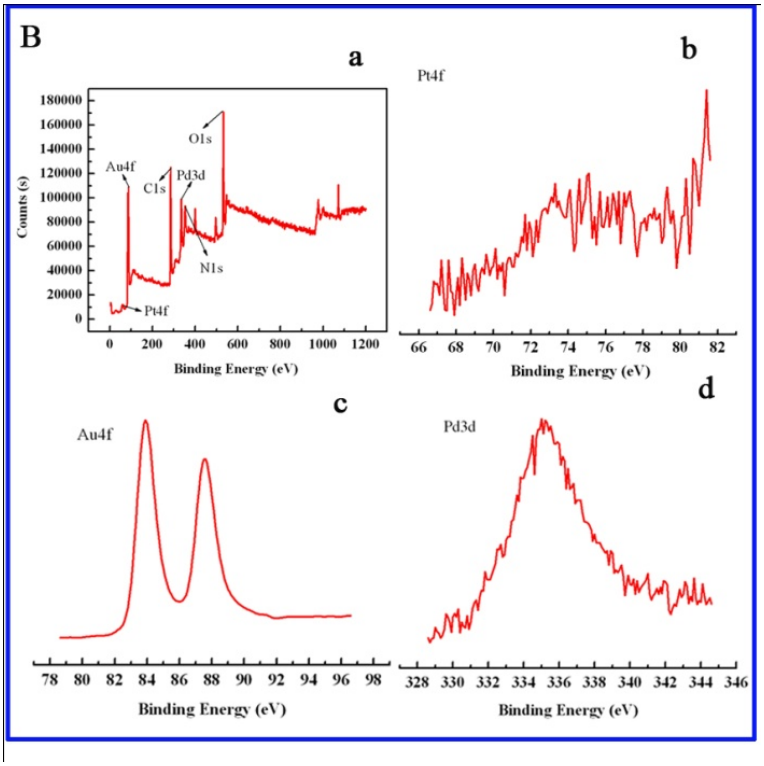

Fig. S1 (A) SEM images of Pd nanocubes (a), Pd-Pt nanocages (b), Pd@Pt/PDA (c), Pd@Pt/PDA/Au (d); (B) XPS spectra of Pd@Pt/PDA/Au nanocomposites (a), and the spectrum of Pt4f (b), Au4f (c), Pd3d (d) in Pd@Pt/PDA/Au nanocomposites.

The electrochemical characterization of the stepwise modified electrode

To further confirm the assemble process of the aptasensor, we employed electrochemical impedance spectroscopy (EIS), one of the most powerful tools for interfacial investigation, to characterize the modified electrodes. Fig. S2 showed the Nyquist plots of impedance spectra at different electrodes. The bare GCE electrode showed a very small semicircle domain (Fig. S2 curve a). Owing to the conductivity of AuNPs, a decrease of semicircle diameter was obtained after the electrochemical deposition of AuNPs (curve b). However, after the consecutive assembling of negative TBA I, inert HT and biological macromolecule TB, the resistances were increased with the stepwise increase of semicircle diameter (curve c, d, e, respectively). The resistance further increased when the electrode was incubated with Pd@Pt/PDA/Au-TBA II-S1-BSA bioconjugates (curve f) and the semicircle diameter

greatly decreased after assembling the MnTMPyP-dsDNA complex (curve g) due to the good electron transfer characteristics of MnTMPyP. The results indicated that a sensing interface was effectively constructed.

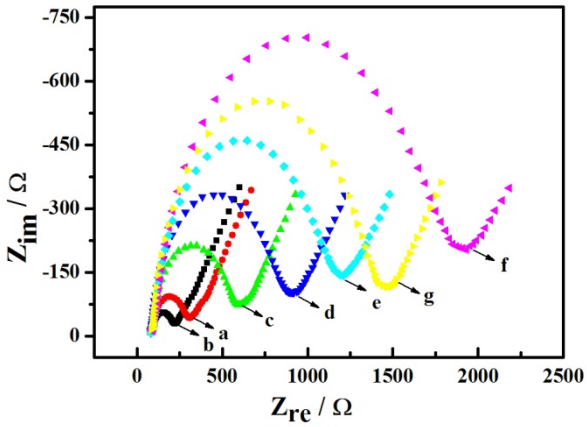

Fig. S2 EIS bare GCE (a); GCE/Au (b); GCE/Au/TBAI (c); GCE/Au/TBAI/HT(d); GCE/Au/TBAI/HT/TB(e); GCE/Au/TBAI/HT/TB/ Pd@Pt/PDA/Au-TBA II-S1-BSA bioconjugates (f); GCE/Au/TBAI/HT/TB/ Pd@Pt/PDA/Au-TBA II-S1-BSA bioconjugates/MnTMPyP-dsDNA (g) in 2 mL 5 mM $K_3[Fe(CN)_6]$ and $K_4[Fe(CN)_6]$ solution containing 0.2 M KCl.

Optimization of aptasensor preparation conditions

In order to obtain a better environmental for polyaniline deposition, experimental parameters such as the incubation time, the H_2O_2 concentration, and the aniline concentration for polymerization were optimized. The effect of PANI deposition time on the biosensor was firstly investigated. As expected in Fig. S3A, with the increasing incubation time, more PANI could be formed and led to the increased peak current. It was clearly observed that the current response increased greatly and trended to level off at 30 min. Therefore, a deposition time of 30 min was selected to ensure the best performance of the biosensor. The optimization of H_2O_2 concentration was carried out in the range of 1-5 mM. The results were depicted in Fig. S3B. The peak current of the PANI increased with increasing H_2O_2 concentration in the range of 1-4 mM, and further increase in H_2O_2 concentration did not show appreciable changes in peak current. Therefore, 4 mM of H_2O_2 was used for subsequent experiments. The effect of

aniline concentration was then studied by varying the aniline concentration in the mixture solution from 0 to 25 mM while keeping the H_2O_2 concentration and the incubation time unchanged. As illustrated in Fig. S3C, no response signal was observed without aniline because of lacking the substance with electrochemical activity. The DPV response signal increased from 5 mM to 20 mM and changed very little after 20 mM. Therefore, 20 mM of aniline was selected to perform PANI deposition, which is high enough to facilitate the longer polymer chain growth.

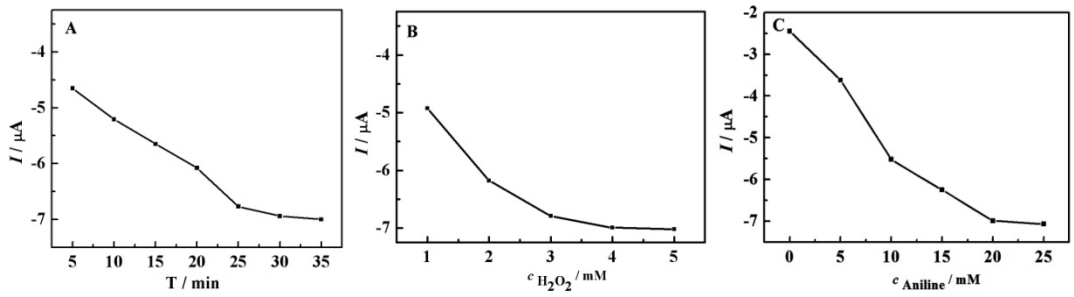

Fig. S3 The optimization of experimental parameters: influence of PANI deposition time on the current response (A); the optimum concentration of H_2O_2 (B); the optimum concentration of aniline (C). Detection buffer: PBS (pH 7.0). All the current signals were detected in the presence of 0.01 nM TB.

The amplification properties of different bioconjugates

In our work, the signal output was achieved by depositing PANI on MnTMPyP-dsDNA complex. It is easy to understand that the more MnTMPyP-dsDNA were formed, the higher peak current were obtained, and the carrier materials played an important role in MnTMPyP-dsDNA assembling. Hence, to verify the amplifying action of the proposed Pd@Pt/PDA/Au-TBA II-S1-BSA bioconjugates, a comparison was made by investigating DPV responses of aptasensor (incubated with 0.01 nM TB) sandwiched with various labeled probes obtained in the same working buffer. Curve a-c in Fig.S4 A displayed the DPV response of MnTMPyP-dsDNA conjugated NanoAu-TBA II-S1-BSA bioconjugates, Pd@Pt-TBAII-S1-BSA bioconjugates and Pd@Pt/PDA/Au -TBA II-S1-BSA bioconjugates, respectively. The electrochemical detection was carried out in an electrolytic cell containing 1 mL 0.1 M PBS (pH 7.0).

As can been seen from Fig.S4 A, the current response of the NanoAu-TBA II-S1-BSA bioconjugates (curve a) was very small, which because of that the immobilized amount of S1 and TBAII on NanoAu were less than the Pd@Pt/PDA/Au nanocomposites as well as the weak catalytic capacity of NanoAu toward the H_2O_2. The Pd@Pt-TBAII-S1-BSA bioconjugates (curve b) showed a higher response than NanoAu-TBA II-S1-BSA bioconjugates, indicating that Pd@Pt nanocages have a positive effect on improving the sensitivity of the aptasensor. As expected, the aptasensor with Pd@Pt/PDA/Au -TBA II-S1-BSA bioconjugates exhibited the maximum response current (curve c), indicating remarkable amplifying performance of the Pd@Pt/PDA/Au nanocomposites. The high peak current of the Pd@Pt/PDA/Au-TBA II-S1-BSA bioconjugates labeled aptasensor may attribute to the following two reasons: First, the resulted Pd@Pt nanocages, which equipped with the characteristics of high catalytic performance and excellent loading capacity, could auxiliary catalyze the reduction of H_2O_2 to produce more polyaniline within a fixed time; Second, the induced PDA and Au nanoparticals could effectively immobilized S1 to form more MnTMPyP-dsDNA *via* HCR. Amine-modified S1 could not only combine with Au nanoparticals, but also graft on the carrier *via* Michael addition between the amine and catechol group of PDA.

The dense MnTMPyP-dsDNA catalyst units on the fabricated “sandwich-type” aptasensor would catalyze the oxidation of aniline to PANI as powerful catalyst and template. To evaluate the specific roles of MnTMPyP-dsDNA, electrochemical responses in the absence of MnTMPyP-dsDNA and MnTMPyP were studied, respectively. As can be seen from Fig S4 B, a low reduction peak current was introduced (curve a) in the system without MnTMPyP-dsDNA, due to the inefficient bioelectrocatalysis and limited surface of Pd@Pt/PDA/Au-BSA-TBA II-S1 bioconjugates for PANI deposition. However, after the system treated with the autonomous assembly of the dsDNA (the system without MnTMPyP), an increase response could be obtained (curve b), suggesting that the negatively charged dsDNA could gather numerous electron mediators PANI to the working electrode, significantly amplified the electrochemical signal. Moreover, when the system treated

with MnTMPyP (the proposed system), the DPV response was further largely increased, indicting the superiority of MnTMPyP-dsDNA electrocatalytic amplification capability as expected.

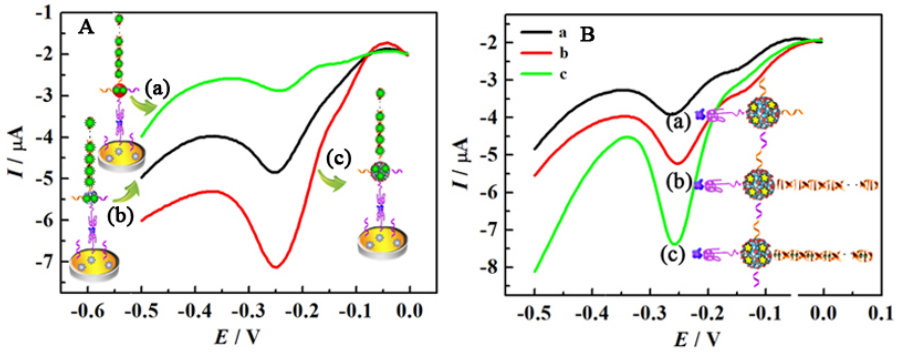

Fig. S4 (A) DPV responses of aptasensor (incubated with 0.01 nM TB) sandwiched with various labeled probes obtained in 0.1 M PBS (pH 7.0): NanoAu-TBA II-S1-BSA bioconjugates (a), Pd@Pt-TBAII-S1-BSA bioconjugates (b) and Pd@Pt/PDA/Au -TBA II-S1-BSA bioconjugates (c). (B) DPV responses of the aptasensor with the deposition of PANI obtained in the electrolyte of PBS. The system without MnTMPyP-dsDNA (a), the system without MnTMPyP (b), and the system proposed in our work (c).

Table S1

Comparisons of detection limit with other detection methodologies as direct thrombin detection

Analytical method	Detection limit	Linear range	Ref.
CV	40 pM	0.12~ 46 nM	3
Fluorescence	67 nM	0.075~12.5 μM	4
SV	22.6 nM	1~500 nM	5
UV-vis	1.5 pM	0.0025~6.2 nM	6
ECL	1 nM	5~200 nM	7
CL	80 pM	0.25~5 nM	8
DPV	0.14 pM	0.0005~ nM	Our work

Abbreviation: cyclic voltammetry (CV); differential pulse voltammetry (DPV); electrochemiluminescent (ECL); UV-vis absorbance measurements (UV-vis); stripping voltammetry (SV); chemiluminescence (CL).

Table S2. Determination of thrombin added in human blood serum (*n=3*) with the proposed aptasensor

Serum sample	Concentration of thrombin added (nM)	Concentration obtained with aptasensor (nM)	Recovery/%	RSD/%
1	0.001	0.001087	108.7	5.45
2	0.01	0.01035	103.5	4.93
3	1	0.952	95.2	5.52
4	30	29.28	97.6	6.78

References

1 G. Frens, Nature-Phys. Sci., 1973, **241**, 20-22.

2 H. Zhang, M.S. Jin, H.Y. Liu, J.G. Wang, M.J. Kim, D. Yang, Z.X. Xie, J.Y. Liu and Y.N. Xia, ACS nano., **10**, 8212-8222.

3 Y. L. Yuan, R. Yuan, Y. Q. Chai, Y. Zhuo, Z. Y. Liu, L. Mao, S. Guan and X. Q. Qian, Anal. Chim. Acta., 2010, **668**, 171-176.

4 L. Zhang, J.P. Lei, L. Liu, C.F. Li, and H.X Ju, Anal. Chem. 2013, **85**, 11077-11082.

5 E. Suprun, V. Shumyantseva, T. Bulko, S. Rachmetova, S. Radko, N. Bodoev and A. Archakov, Biosens. Bioelectron., 2008, **24**, 825.

6 Y. Huang, J. Chen, S.L Zhao, M. Shi, Z.F. Chen and H. Liang, Anal. Chem., 2013, **85**, 4423-4430.

7 P. Zhao, L.F. Zhou, Z. Nie, X.H. Xu, W. Li, Y. Huang, K.Y. He and S.Z. Yao, Anal. Chem., 2013, **85**, 6279-6286.

8 Z. Jiang, T.T. Yang, M.Y. Liu, Y.L. Hua, J. Wang, Biosens. Bioelectron., 2014, **53**, 340-345.